9912 *Biochemistry* **2009,** *48,* 9912–9920
DOI: 10.1021/bi9012098

BIOCHEMISTRY
including biophysical chemistry & molecular biology
Article

Why the Extended-Spectrum β-Lactamases SHV-2 and SHV-5 Are "Hypersusceptible" to Mechanism-Based Inhibitors†

Matthew Kalp,‡ Christopher R. Bethel,‖ Robert A. Bonomo,§,‖ and Paul R. Carey*,‡

‡*Department of Biochemistry and* §*Departments of Pharmacology, Molecular Biology and Microbiology, and Medicine, Case Western Reserve University, 10900 Euclid Avenue, Cleveland, Ohio 44106, and* ‖*Research Service, Louis Stokes Cleveland Veterans Affairs Medical Center, Cleveland, Ohio 44106*

Received July 15, 2009; Revised Manuscript Received September 6, 2009

ABSTRACT: Extended-spectrum β-lactamases (ESBLs) are derivatives of enzymes such as SHV-1 and TEM-1 that have undergone site-specific mutations that enable them to hydrolyze, and thus inactivate, oxyimino-cephalosporins, such as cefotaxime and ceftazidime. X-ray crystallographic data provide an explanation for this in that the mutations bring about an expansion of the binding pocket by moving a β-strand that forms part of the active site wall. Another characteristic of ESBLs that has remained enigmatic is the fact that they are "hypersusceptible" to inhibition by the mechanism-based inactivators tazobactam, sulbactam, and clavulanic acid. Here, we provide a rationale for this "hypersusceptibility" based on a comparative analysis of the intermediates formed by these compounds with wild-type (WT) SHV-1 β-lactamase and its ESBL variants SHV-2 and SHV-5, which carry the G238S and G238S/E240K substitutions, respectively. A Raman spectroscopic analysis of the reactions in single crystals shows that, compared to WT, the SHV-2 and SHV-5 variants have relatively higher populations of the stable *trans*-enamine intermediate over the less stable and more easily hydrolyzable *cis*-enamine and imine co-intermediates. In solution, SHV-2 and SHV-5 also form larger populations of an enamine species compared to SHV-1 as detected by stopped-flow kinetic experiments under single-turnover conditions. Moreover, a simple Raman band shape analysis predicts that the *trans*-enamine intermediates themselves in SHV-2 and SHV-5 are held in more stable, rigid conformations compared to their *trans*-enamine analogues in WT SHV-1. As a result of this stabilization, more of the *trans*-enamine intermediate is formed, which subsequently lowers the K_I values of the mechanism-based inhibitors up to 50-fold in SHV-2 and SHV-5.

Extended-spectrum β-lactamase-producing Gram-negative organisms are a growing cause of healthcare-associated infections. *Escherichia coli*, *Klebsiella pneumoniae*, and *Proteus* spp. are the most common extended-spectrum β-lactamase-producing pathogens recognized in the United States (*1*). The widespread use of oxyimino-cephalosporins, which were introduced in the 1980s to treat antibiotic-resistant bacteria, is believed to be a major contributor to the emergence of extended-spectrum β-lactamase-producing organisms. Extended-spectrum β-lactamase-producing organisms are able to hydrolyze oxyimino-cephalosporins and monobactams (Scheme 1, top); moreover, extended-spectrum β-lactamase-producing organisms are generally resistant to aminoglycosides because the *bla* genes that encode ESBLs[1] are carried on mobile elements that also carry other antibiotic resistance factors, such as genes encoding aminoglycoside-modifying enzymes. As a result, it is necessary for clinical laboratories to detect the production of ESBLs in order for clinicians to initiate appropriate antibiotic therapy (*2*). Carbapenems (imipenem, meropenem, ertapenem, and doripenem) are stable against hydrolysis by ESBLs and are regarded as the "drugs of choice" for infections due to ESBL-producing organisms (*3*, *4*).

The first plasmid-mediated β-lactamase capable of hydrolyzing extended-spectrum cephalosporins, now known as SHV-2, was reported in 1983, and a number of other groups of β-lactamases with expanded hydrolytic activity were reported thereafter (*5*, *6*). The term "extended-spectrum β-lactamase" was applied to denote these enzymes with activity against extended-spectrum cephalosporins, such as cefotaxime, ceftazidime (Scheme 1), ceftriaxone, and cefuroxime (*7*−*9*). Sequencing of the encoding genes revealed that most ESBLs described in the 1980s were derived from genes for bla_{TEM-1} or bla_{SHV-1} by mutations that alter the architecture of the active site. The current emergence of CTX-M-type ESBLs, β-lactamases whose substrate profile favors either cefotaxime or ceftazidime hydrolysis, is also becoming an international problem (*4*, *10*, *11*). The latter family of ESBLs is now found in many isolates of *E. coli* that are responsible for community-acquired urinary tract infections.

In both SHV and TEM backgrounds, the G238S substitution is critical for cefotaxime hydrolysis, whereas both the G238S and E240K substitutions are needed for clinically significant ceftazidime hydrolysis (*12*, *13*). An overlay of either the SHV G238S or TEM G238S crystal structure with the respective WT crystal

†This work was supported in part by National Institutes of Health (NIH) Grant RO1 GM54072 (P.R.C.), NIH Grant 1RO1 A1063517-01 (R.A.B.), the Department of Veterans Affairs Merit Review Program (R.A.B.), VISN 10 GRECC (R.A.B.), and the Case Western Reserve University MSTP Program (M.K.).

*To whom correspondence should be addressed. E-mail: paul.carey@case.edu. Telephone: (216) 368-0031. Fax: (216) 368-3419.

[1]Abbreviations: ESBL, extended-spectrum β-lactamase; WT, wild-type; TEM, class A β-lactamase of *E. coli* first described in a Greek patient, with the name being derived from the patient's name; SHV, class A β-lactamase of *K. pneumoniae* initially thought to be a "sulfhydryl variant" of the TEM enzyme; MES, 2-(4-morpholino)ethanesulfonic acid; HPLC, high-performance liquid chromatography; MIC, minimal inhibitory concentration.

 Published on Web 09/08/2009

Scheme 1

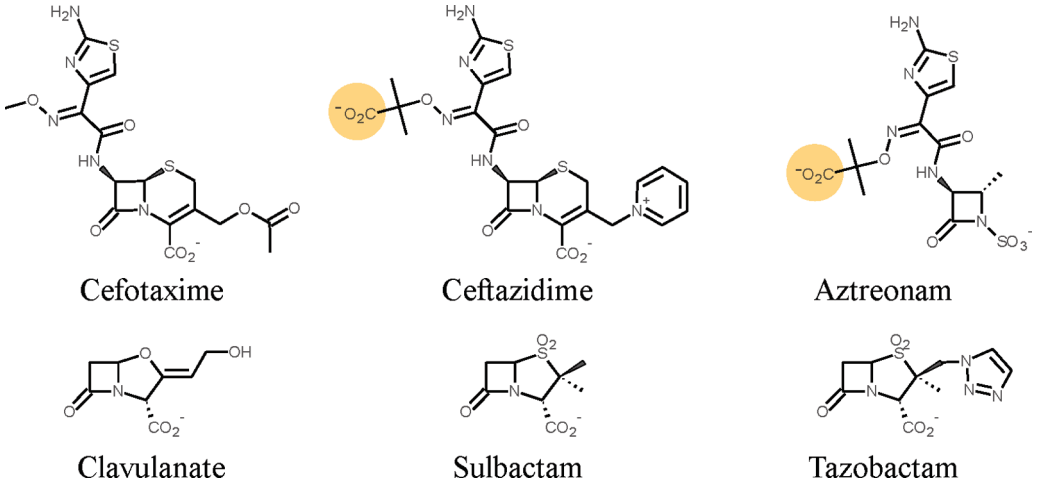

Scheme 2: Reaction Scheme for Sulbactam and Serine 70 in the Active Site of a β-Lactamase[a]

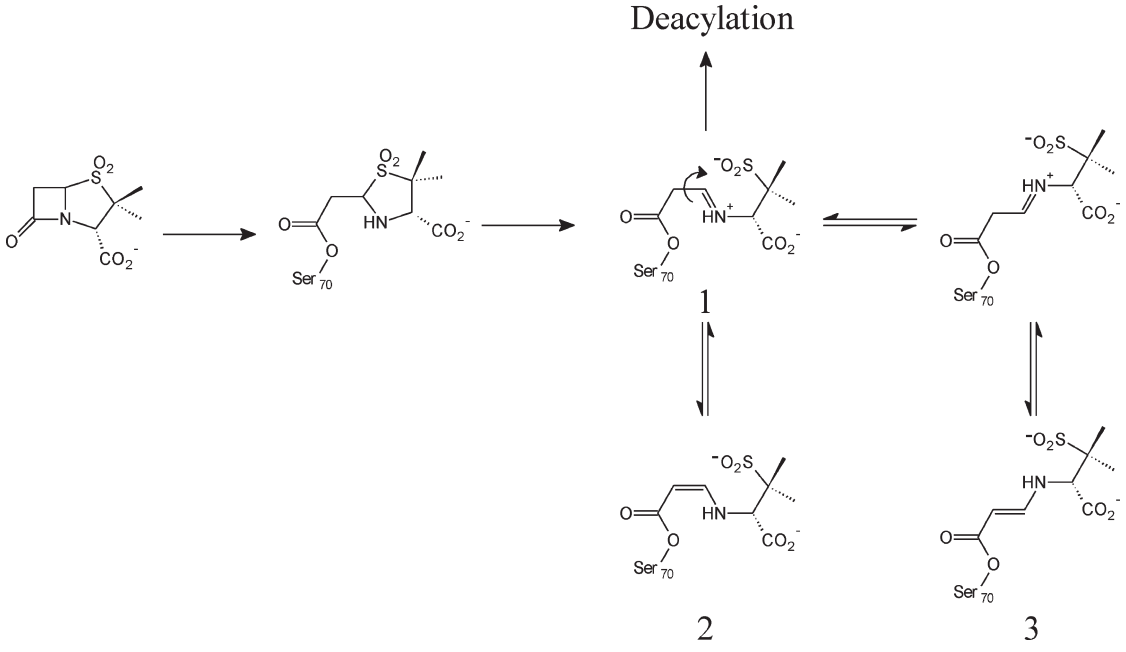

[a] **1** is an imine, and **2** and **3** are *cis*- and *trans*-enamines, respectively. In addition to deacylation, the imine (**1**) can be attacked by S130 to yield an acrylate-like species.

structure shows a significant 1−3 Å displacement in the β-strand−turn segment (residues 238−242), which allows the β-lactam binding site to accommodate oxyimino-cephalosporins with large C7 groups, thereby expanding the substrate spectrum of the variant enzyme (*14*, *15*). The E240K substitution is observed only in concert with either the G238S or R164S substitution and confers an enhanced ability to hydrolyze ceftazidime and aztreonam, which both possess a bulky 1-carboxy-1-methylethoxyimino side chain (highlighted in Scheme 1). Unlike the G238S substitution, structural data are not available for either TEM or SHV E240K; however, molecular modeling suggests that the lysine side chain is able to form an electrostatic bond with the carboxylic acid of the oxyimino substituent (highlighted in Scheme 1) (*13*). If residue 240 is glutamate, as in WT or G238S, its carboxylic acid group encounters the oxime's carboxylic acid group. Consequently, the electrostatic repulsion results in little catalytic activity against either ceftazidime or aztreonam (*13*).

Another distinguishing and unexplained attribute of ESBLs is their "hypersusceptibility" to mechanism-based inhibitors, such as sulbactam, tazobactam, and clavulanic acid (Scheme 1, bottom) (*16*). Following an attack on the β-lactam carbonyl by the S70 side chain, the resultant acyl−enzyme intermediate undergoes a series of proton transfers in which a variety of intermediates, including imine **1**, *cis*-enamine **2**, *trans*-enamine **3**, and irreversible S130-bound acrylate (not shown), are possible (see Scheme 2). Mechanistically, the linear *trans*-enamine intermediate is a long-lived inhibitory species (*17*−*19*). Consequently, the hypersusceptibility of SHV-type ESBLs, compared to the WT enzyme, may arise from relative or absolute differences in the amount of *trans*-enamine formed by a given inhibitor. Previous Raman and X-ray analysis of an inhibitor-resistant β-lactamase showed that addition of the M69V mutation to an E166A background reduced the amount of *trans*-enamine seen with tazobactam and clavulanic acid (*20*). While significant structural changes were not seen in the binding of the *trans*-enamine

intermediate once it was formed, X-ray crystallography detected a slightly smaller oxyanion hole for the M69V/E166A variant (*20*). In this work, potential differences in inhibitory population levels were explored in single crystals of SHV-2 or -5 by Raman microscopy, which detects larger relative amounts of the *trans*-enamine acyl−enzyme intermediate compared to SHV-1. Additionally, UV spectroscopy in solution shows that, under single-turnover conditions, SHV-2 and SHV-5 make approximately 35% more of an enamine-type species than SHV-1. Higher populations of the *trans*-enamine intermediate result in lower K_I values and greater inactivation efficiencies for the mechanism-based inhibitors compared to the WT enzyme. Together, the data explain the observed in vivo and in vitro hypersusceptibility of ESBLs harboring mutations in the key β-strand of the catalytic site of class A β-lactamases.

MATERIALS AND METHODS

Bacterial Strains and Plasmids. β-Lactamase genes encoding bla_{SHV-1}, bla_{SHV-2}, and bla_{SHV-5} were cloned into the pBC SK(−) phagemid vector (Stratagene, La Jolla, CA) as previously described (*21*). The β-lactamases were expressed in *E. coli* DH10B cells (Invitrogen, Carlsbad, CA), liberated by stringent periplasmic fractionation, and initially purified by preparative isoelectric focusing (*21*). The β-lactamases were further purified by size exclusion chromatography using a Waters high-performance liquid chromatography (HPLC) system. The purity of each β-lactamase was assessed via 5% stacking and 12% resolving sodium dodecyl sulfate polyacrylamide gel electrophoresis. Gels were stained with Coomassie Brilliant Blue R250 (Fisher) to visualize the β-lactamases. Protein concentrations were determined by a standard Bradford assay (Bio-Rad) using bovine serum albumin as a standard.

Antibiotic Susceptibility Testing. *E. coli* DH10B cells expressing the bla_{SHV} genes were phenotypically characterized by lysogeny broth agar dilution minimum inhibitory concentrations (MICs) using a "Steers replicator" that delivered 10^4 colony forming units per spot (*21*). Concentrations employed for determining MIC values were in micrograms per milliliter. MICs were read after incubation for 18−24 h at 37 °C and determined three times for each antibiotic. Ampicillin, ceftazidime, and cefotaxime were obtained from Sigma-Aldrich Chemical Co. Nitrocefin was obtained from CalBioChem (San Diego, CA). Sodium clavulanate (Smith-Kline-Beecham), sulbactam (Pfizer), and tazobactam (Wyeth Pharmaceuticals) were gifts of the respective companies.

Kinetics. Steady-state kinetics were determined using continuous assays at room temperature in an Agilent (Palo Alto, CA) 8453 diode array spectrophotometer. Each assay was performed in 10 mM phosphate-buffered saline (PBS) at pH 7.4. Measurements were taken using nitrocefin (NCF) (BD Biosciences, San Jose, CA) ($\Delta\varepsilon_{482}$ = 17400 M^{-1} cm^{-1}).

The kinetic parameters, V_{max} and K_M, were obtained with a nonlinear least-squares fit of the data (Henri Michaelis−Menten equation) using Origin 7.5 (OriginLab, Northampton, MA):

$$v = (V_{max}[S])/(K_M+[S]) \quad (1)$$

For each of the β-lactamase inhibitors, the K_I values (equivalent to K_M) were determined by direct competition assays. The initial velocity was measured in the presence of a constant concentration of enzyme (10 nM) with increasing concentrations of inhibitor against the indicator substrate, NCF. Care was taken to initiate the reaction with the addition of both NCF and the inhibitor and to limit the initial velocity determination to the first 5 s. The K_I data were corrected to account for the affinity of NCF for SHV-1, SHV-2, and SHV-5 according to the following equation:

$$K_I(\text{corrected}) = K_I(\text{observed})/[1+[S]/K_{M(NCF)}] \quad (2)$$

The first-order rate constant for enzyme and inhibitor complex inactivation, k_{inact}, was obtained by monitoring the reaction time courses in the presence of inhibitor. Fixed concentrations of enzyme (10 nM) and NCF (150 μM) and increasing concentrations of inhibitor were used in each assay. The k_{obs} was determined using a nonlinear least-squares fit of the data using Origin 7.5:

$$A = A_0+v_f t+(v_0-v_f)[1-\exp(-k_{obs}t)]/k_{obs} \quad (3)$$

where A is absorbance, v_0 (expressed in variation of absorbance per unit time) is initial velocity, v_f is final velocity, and t is time. Each k_{obs} was plotted versus I and fit to determine k_{inact}.

Stopped-flow ultraviolet absorbance analysis was performed on an Applied Photophysics π* 180 spectrometer. Reactions were performed in 10 mM phosphate-buffered saline (PBS) at pH 7.4. The temperature was regulated at 25.0 ± 0.1 °C using a circulating water bath. Reactions were initiated by injecting equal volumes of tazobactam and either SHV-1, SHV-2, or SHV-5 into a flow cell. After the solution had been mixed, the final concentration of both the enzyme and the substrate was 2 μM. Absorbance measurements were recorded at 288 nm using a variable-wavelength monochromator and a 75 W mercury−xenon light source.

Crystallization. Initial crystallization screens were conducted using the sitting-drop vapor-diffusion method in 96-well plates. Sitting-drop procedures were conducted by mixing equal volumes of a 5 mg/mL protein solution and crystallizing solution from Crystal Screen 1 and 2 (Hampton Research, Laguna Niguel, CA). Small plates were obtained from solution 20 in Crystal Screen 1 [0.1 M MES (pH 6.5) and 1.6 M $MgSO_4 \cdot 6H_2O$]. Following addition of 5.6 mM CYMAL-6 (Hampton Research) to the crystallizing solution, larger crystals were obtained from hanging drops after approximately 2 weeks. The resulting crystals belong to space group $P2_12_12_1$ (J. Sampson and F. van den Akker, personal communication).

Raman Crystallography. The Raman microscope system has been described previously (*22*). A 647 nm Kr^+ laser beam (Innova 70 C, Coherent, Palo Alto, CA) was focused onto the protein crystals, suspended on the underside of a siliconized quartz coverslip in a 4 μL drop. Laser power (120 mW) was focused using the 20× objective to a 20 μm spot on the crystal. The crystals and the laser spot were visualized with video display to ensure alignment with the focal spot of the laser. During data collection, spectra were acquired over 10 s intervals and 10 spectra were averaged for each acquisition time point. Spectra of the apo-β-lactamase protein crystals were obtained, followed by addition of the inhibitors to the drop, yielding a final drop volume of 4 μL and a final inhibitor concentration of 5−10 mM. Spectra were then recorded serially every 2−3 min following addition of inhibitor. An apo-β-lactamase spectrum was subtracted from the inhibited protein spectra at varying time intervals following addition of inhibitor:

$$\text{difference spectrum} = [\text{protein+inhibitor}]-[\text{protein}] \quad (4)$$

Data collection and subtractions were performed using HoloGRAMS and GRAMS/AI 7 (ThermoGalactic, Inc., Salem,

Table 1: MICs for the DH10B Strain Alone and Producing SHV-1, SHV-2 (G238S), or SHV-5 (G238S/E240K)

(A)

	MIC (μg/mL)	
	ampicillin	piperacillin
DH10B	1	2
SHV-1	> 16382	2048
SHV-2	8192	512
SHV-5	16384	512

(B)

	MIC (μg/mL)	
	ceftazidime	cefotaxime
DH10B	1	0.25
SHV-1	2	0.25
SHV-2	8	16
SHV-5	> 128	32

(C)

	MIC (μg/mL)		
	ampicillin/ tazobactam	ampicillin/ sulbactam	ampicillin/ clavulanic acid
DH10B	1	1	1
SHV-1	128	512	2
SHV-2	8	16	1
SHV-5	8	16	1

NH). Raman spectra of the inhibitors that were used were recorded under similar conditions. Spectra were obtained for 4 μL drops of 100 mM inhibitor solutions prepared in 2 mM HEPES (pH 7.0).

Band Fitting of the Raman Spectra. The conformational heterogeneity of the *trans*-enanine intermediates of tazobactam and clavulanic acid was investigated by analyzing the O=C−C=C−NH stretch of the *trans*-enamine Raman band. The extended enamine region (1575−1645 cm^{-1}) was fitted assuming three component bands that represent a *cis*-enamine band near 1585 cm^{-1}, a *trans*-enamine band near 1600 cm^{-1}, and an antisymmetric stretch of the C3 carboxylate near 1630 cm^{-1} (*23*). Component bands were fitted by 15−35 cm^{-1} bandwidth features; Gaussian and Lorentzian functions were employed as models of homogeneous and heterogeneous broadening, respectively. Fitting was performed using the Levenberg−Marquardt nonlinear least-squares method as implemented in the CurveFit.Ab routine of GRAMS/32. The baseline was taken as a linear function. The standard error for peak positions is < 1 cm^{-1} and for peak widths < 2 cm^{-1} for well-defined components, such as the *trans*-enamine band.

RESULTS AND DISCUSSION

Antibiotic Susceptibility. To assess the impact of the amino acid substitutions on the behavior of SHV β-lactamase in *E. coli* DH10B, we first determined the MICs. *E. coli* DH10B cells containing bla_{SHV-1} encoded in the pBC SK(−) phagemid vector exhibit robust levels of resistance to ampicillin (MIC ≥ 16000 μg/mL) and piperacillin (MIC = 2049 μg/mL). However, for both SHV-2 and SHV-5, ampicillin and piperacillin MICs were decreased by up to four dilutions compared to WT SHV-1 containing *E. coli* strains (Table 1A).

Table 2: Steady-State Kinetic Parameters

	clavulanic acid	sulbactam[a]	tazobactam
K_I (μM)			
SHV-1	1 ± 0.04	8.6 ± 0.7	0.200 ± 0.035
SHV-2	0.330 ± 0.030	0.490 ± 0.050	0.030 ± 0.003
SHV-5	0.158 ± 0.013	0.200 ± 0.016	0.019 ± 0.001
K_{inact} (s^{-1})			
SHV-1	0.04 ± 0.02		0.14 ± 0.01
SHV-2	0.05 ± 0.01		0.030 ± 0.003
SHV-5	0.06 ± 0.01		0.025 ± 0.001
k_{inact}/K_I (μM^{-1} s^{-1})			
SHV-1	0.04 ± 0.03		0.70 ± 0.12
SHV-2	0.15 ± 0.03		1.00 ± 0.14
SHV-5	0.38 ± 0.07		1.32 ± 0.10

[a]Because of the rapid hydrolysis of sulbactam by both the WT and extended-spectrum β-lactamases, values for k_{inact} could not be determined. Consequently, the K_i values rather than the K_I values are given. See Materials and Methods for further details.

For *E. coli* expressing SHV-1 β-lactamase, MICs for cefotaxime (0.25 μg/mL) and ceftazidime (2 μg/mL) were similar to control cells (Table 1B). While both the G238S and G238S/E240K variants conferred levels of resistance to cefotaxime significantly higher than that of the parent enzyme (MIC = 16 and 32 μg/mL, respectively), only the G238S/E240K double substitution resulted in high-level resistance to ceftazidime (MIC ≥ 128 μg/mL).

The results listed in Table 1B confirm that while SHV-2 and SHV-5 have activity toward cefotaxime and ceftazidime, they are also "hypersusceptible" to the clinical inhibitors sulbactam, tazobactam, and clavulanic acid. Currently, the use of β-lactam antibiotics in combination with β-lactamase inhibitors represents a potentially effective measure for combating a specific resistance mechanism of some β-lactamase-producing organisms. Compared to the WT-producing strain, *E. coli* DH10B containing either SHV-2 or SHV-5 was more susceptible to β-lactam/β-lactamase inhibitor combinations. For both ESBL variants, susceptibility to these combinations was reduced by one dilution for ampicillin and clavulanic acid (MIC = 50 and 1 μg/mL, respectively), four dilutions for ampicillin and sulbactam (MIC = 50 and 16 μg/mL, respectively), and five dilutions for ampicillin and tazobactam (MIC = 50 and 8 μg/mL, respectively) compared to the wild type (Table 1C).

Kinetic Behavior of Hypersusceptible β-Lactamases with the Mechanism-Based Inhibitors. Next, we show that the observed decrease in antibiotic susceptibility of *E. coli* cells containing either bla_{SHV-2} or bla_{SHV-2} to tazobactam, sulbactam, and clavulanic acid results from only minor changes in the steady-state kinetic parameter (K_I, k_{inact}, and K_I/k_{inact}). A common feature of hypersusceptible enzymes SHV-2 and SHV-5 is a decrease by less than 1 order of magnitude for clavulanate and tazobactam and of 20−50-fold for sulbactam in the K_I values for the mechanism-based inhibitors (Table 2). With clavulanate, both the WT and hypersusceptible enzymes exhibited similar k_{inact} values. Consequently, the decreased K_I of these variant enzymes for clavulanate is solely responsible for their increased inactivation efficiency (k_{inact}/K_I). In contrast, the WT enzyme exhibited an increased k_{inact} value with tazobactam compared to SHV-2 and SHV-5; however, the inactivation efficiency (k_{inact}/K_I) of the ESBLs was still increased slightly over the

wild-type value (Table 2). Sulbactam was rapidly hydrolyzed by both the WT and extended-spectrum β-lactamases. As a result, values for k_{inact} could not be determined. Despite the increased inactivation efficiencies of β-lactamase inhibitors against SHV-2 and SHV-5, the effects are less than 1 order of magnitude. Because sulbactam, tazobactam, and clavulanate follow a multistep reaction pathway, we next examined the relative populations of the inhibitory intermediates formed with each β-lactamase to explain the kinetic data and antibiotic susceptibilities.

Clinical Inhibitors Form a Predominant Population of the trans-Enamine with SHV-2 and SHV-5. In the following sections, we present evidence using Raman crystallography that, compared to wild-type SHV-1, the clinical inhibitors form measurably larger populations of the hydrolytically inert *trans*-enamine with the ES β-lactamases, SHV-2 and SHV-5. Moreover, we show that the *trans*-enamine acyl−enzyme intermediates of ES β-lactamases are held in a rigid and nonflexible conformation, which may increase their stability and which can be attributed, at least in part, to a conformational change in the β-strand segment of residues 238−242. The Raman difference spectra of the clinical inhibitors with a deacylation-deficient E166A mutant and the wild-type enzyme are provided for comparison. For the sake of brevity, only the SHV-2 difference spectra are shown. The SHV-5 difference spectra are nearly identical to those of SHV-2 and appear in the Supporting Information.

Sulbactam. The difference spectra of the acyl−enzyme intermediate populations of sulbactam with E166A, SHV-1, and SHV-2 are shown in Figure 1a−c. The Raman spectrum of the *trans*-enamine species formed by sulbactam with E166A β-lactamase is shown in Figure 1a and discussed at length by Helfand et al. (*17*). A predominant *trans*-enamine species is identified in the active site, with a Raman signature peak near 1600 cm^{-1} from the stretching motions of the O=C−C=C−NH moiety. There are minor contributions in the E166A−sulbactam difference spectra from both the imine (1654 cm^{-1}) and *cis*-enamine, which displays a shoulder near 1590 cm^{-1}. In previous studies, we determined that the maximum amount of *trans*-enamine intermediate was attained within 20−30 min, which permitted us to identify the conditions needed for optimizing the *trans*-enamine populations in single crystals for flash-freezing and for colleagues to obtain high-resolution crystal structures (*17*−*19*). The SHV-1−sulbactam difference spectrum is shown in Figure 1b. Unlike the case for E166A, it is immediately obvious that sulbactam does not form a predominant population of *trans*-enamine with the wild-type enzyme. The conjugated O=C−C=C−NH stretch of the *trans*-enamine at 1606 cm^{-1} and a peak of similar intensity at 1588 cm^{-1}, which is assigned to the O=C−C=C−NH stretch of the *cis*-enamine, indicate nearly equal populations from the *cis*- and *trans*-enamine acyl−enzyme intermediates at steady state. The *cis*/*trans*-enamine vibrations couple with the antisymmetric CO_2^- stretch to give an unresolved medium-intensity band near 1630 cm^{-1}. Additionally, the 1654 cm^{-1} band is assigned to the C=NH^+ stretch of the imine acyl−enzyme intermediate. Thus, with sulbactam, SHV-1 difference spectra show evidence of a mixture of *trans*- and *cis*-enamine and an imine population in which, compared to E166A, there is a relatively smaller amount of *trans*-enamine. The deuterium isotope exchange experiments, ab initio calculations, and model systems that were used to assign the *cis*-enamine and imine bands are presented by Kalp et al. (*23*). Lastly, the intermediate acyl−enzyme intermediate populations of sulbactam with the

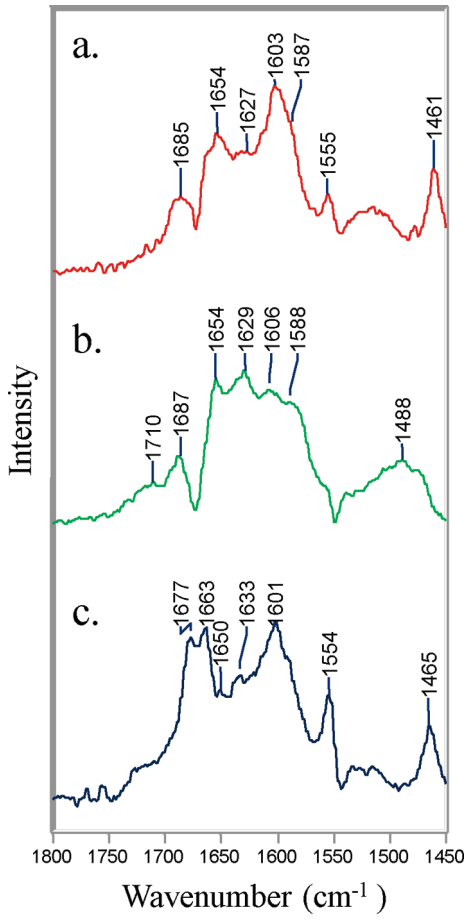

FIGURE 1: Partial Raman difference spectra of sulbactam reacting in crystals of three β-lactamases: (a) SHV E166A, (b) wild-type SHV-1, and (c) SHV-2, which carries the G238S substitution.

hypersusceptible variant, SHV-2, are shown in Figure 1c. With the exception of the intense doublet at 1677 and 1663 cm^{-1}, the spectrum closely resembles the E166A−sulbactam difference spectra. The band seen at 1554 cm^{-1} is due to a tryptophan ring mode. Again, a predominant population of the *trans*-enamine species is identified in the active site, with a Raman signature peak at 1601 cm^{-1}. Compared to that of SHV-1, the Raman difference spectra of the acyl−enzyme intermediates formed between sulbactam and SHV-2 or E166A show a relative increase in the *trans*-enamine population. This indicates that SHV-2 and E166A selectively stabilize the *trans*-enamine and slow its tautomerization to the hydrolysis-prone imine. The resonance-stabilized vinylogous urethane is common to both the *cis*- and *trans*-enamine and deactivates them to hydrolytic deacylation; however, *cis*−*trans* isomerization is favored to due to the intrinsic steric clash of the *cis* form. Isomerization occurs via the common imine, which is hydrolytically labile because of the lack of conjugation with the acyl carbonyl group. As a result, enzymes, such as SHV-1, that have a major population of *cis*-enamine (and thus imine) are not as effectively inhibited by sulbactam. This is reiterated by both the MIC values (Table 1C) and the kinetic data (Table 2).

Clavulanic Acid. As we have reported previously, the *trans*-enamine is the sole acyl−enzyme intermediate formed when clavulanic acid is reacted with E166A β-lactamase crystals (*17*). A high-resolution structure confirmed that the *trans*-enamine of clavulanic acid was bound to E166A with nearly 100% occupancy (*18*). Accordingly, the Raman spectrum of this species

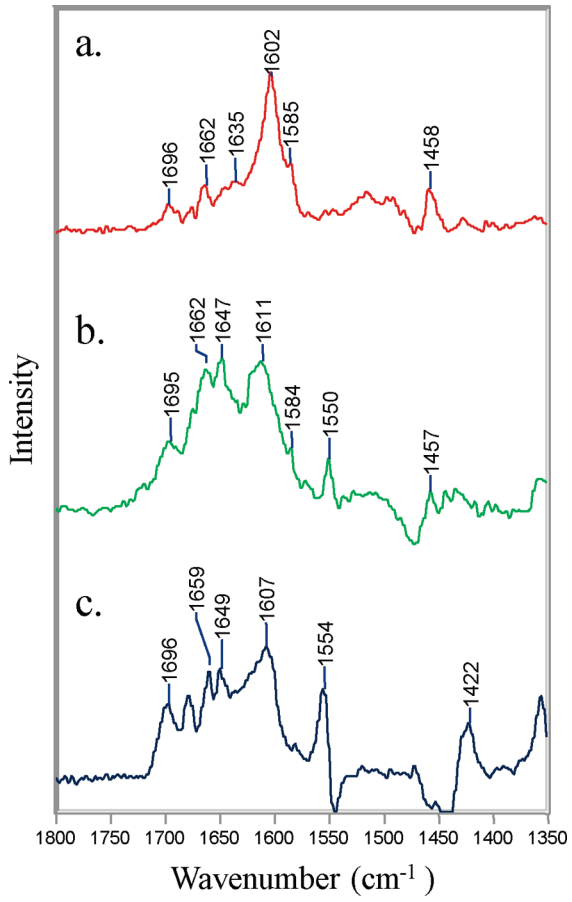

FIGURE 2: Partial Raman difference spectra of clavulanic acid reacting in crystals of three β-lactamases: (a) SHV E166A, (b) wild-type SHV-1, and (c) SHV-2.

Scheme 3: Imine Tautomers Formed after Acylation of the Active-Site Serine by Clavulanic Acid

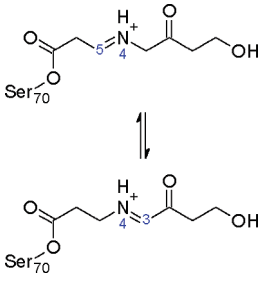

demonstrates a single band at 1602 cm^{-1} (Figure 2a). Analysis of our previously published Raman difference spectra indicated that all three inhibitors, free in solution, have a medium-intensity Raman mode near 1400 cm^{-1}, which is due to the symmetric stretching vibration of the CO_2^- group (*17*, *23*). For the bound tazobactam and sulbactam, this feature shifts to ~1375 cm^{-1}, reflecting electrostatic interactions of the CO_2^- group with active site residues. For clavulanic acid bound to E166A, however, there was no peak in this region, which suggested that the CO_2^- group was no longer present (*17*). This observation was also confirmed by X-ray crystallography (*23*). When clavulanic acid is reacted with the wild-type enzyme, two additional bands are noted in the difference spectrum at 1662 and 1647 cm^{-1} (Figure 2b). These bands have been assigned to a tautomer pair of imine acyl−enzyme intermediates (Scheme 3) (*23*). The 1662 cm^{-1} band in the SHV-1−clavulanate complex is assigned to a C5=N4 imine that results from cleavage of the C−O bond and concomitant opening of the oxazolidinium ring. Structurally, this imine is analogous to those formed by sulbactam and tazobactam. Tautomerization of the C5=N4 imine to the N4=C3 imine is driven by resonance with the adjacent ketone at C2. The N4=C3 imine, which is marked by the 1647 cm^{-1} band in the Raman spectrum, is unique to clavulanate and was first detected by mass spectrometry (*24*). Assignments of the imine bands, reported by Kalp et al. (*23*), are based on their frequency in the Raman spectra, QM calculations, response to NH−ND exchange, and response to reduction by sodium cyanoborohydride, a reducing reagent that is specific for protonated imines (*23*). In addition, clavulanate may generate a minor population of *cis*-enamine; like sulbactam, the 1585 cm^{-1} shoulder features of both the E166A and SHV-1 difference spectra are assigned to the *cis* O=C−C=C−NH stretch. The clavulanate−SHV-2 difference spectrum, shown in Figure 2c, is similar to the wild-type difference spectrum with one notable exception: Clavulanic acid forms a greater amount of *trans*-enamine relative to imine with SHV-2 than with SHV-1. Because the *trans*-enamine is responsible for transient inhibition of the enzyme, a β-lactamase that stabilizes this intermediate, such as SHV-2, will be more susceptible to mechanism-based inhibitors than a β-lactamase, such as SHV-1, which forms relatively more of the hydrolysis-prone imine.

Tazobactam. Tazobactam possesses superior in vivo and in vitro efficacy against SHV β-lactamases when compared to sulbactam or clavulanic acid. Unlike the other inhibitors, tazobactam forms a predominant population of *trans*-enamine with both SHV E166A and WT SHV-1 β-lactamases. In the Raman difference spectra, the O=C−C=C−NH stretch of the *trans*-enamine appears as a relatively intense band between 1593−1596 cm^{-1} (Figure 3). One notable exception between the E166A and wild-type difference spectra is the presence of a sharp band at 1658 cm^{-1} in the latter. This band is assigned to the $C{=}NH^+$ stretch of a protonated imine species and represents a population of hydrolysis-prone acyl−enzyme intermediates. There is little if any contribution from the $C{=}NH^+$ stretch of the imine to the tazobactam−E166A difference spectrum. The tazobactam-bound difference spectrum obtained with SHV-2 is shown in Figure 3c. Aside from bands at 1663 and 1677 cm^{-1} that result from protein conformational changes, the spectrum is very similar those presented in Figure 3a,b. One small difference is the decreased intensity of the imine's $C{=}NH^+$ stretch at 1658 cm^{-1} in the tazobactam−SHV-2 difference spectrum (Figure 3c) compared to the WT SHV-1 spectrum (Figure 3b). Although this change is difficult to observe because of the surrounding interference from the protein bands, it is reproducible. In addition to changes in imine population, there is another factor that may operate to provide the hypersusceptibility of ES β-lactamases to mechanism-based inhibitors.

Next, we present evidence that SHV-2 and SHV-5 form *trans*-enamine intermediates in potential minima which are more well-defined than their "floppy" counterparts in SHV-1. This evidence comes from a comparison of the *trans*-enamine peak widths of tazobactam and clavulanic acid in several different SHV β-lactamases: the deacylation-deficient variant, SHV E166A; two ESBLs, SHV-2 and SHV-5; and wild-type SHV-1 at 4 °C and room temperature. After analyzing the individual difference spectra at 20 min, the following order of increasing *trans*-enamine bandwidths at half-height was found for both tazobactam and clavulanic acid: SHV E166A < SHV-2 < SHV-5 < SHV-1 (4 °C) < SHV-1 (Figure 4). In the Raman spectroscopic

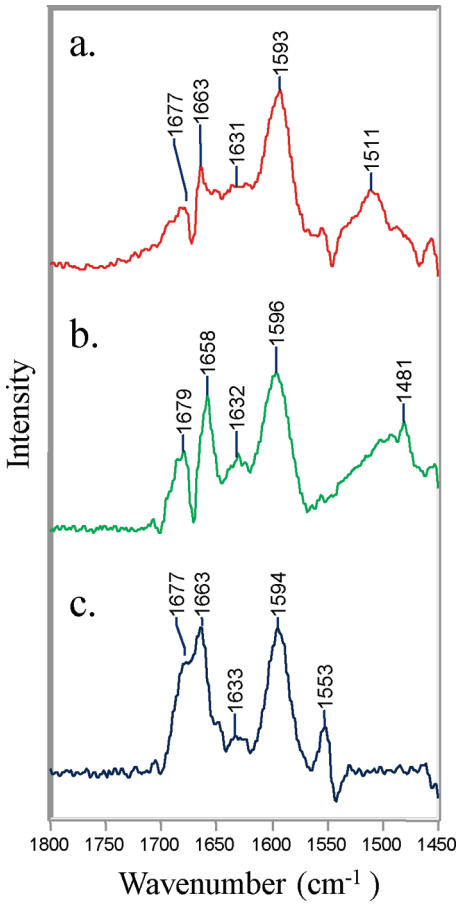

FIGURE 3: Partial Raman difference spectra of tazobactam reacting in crystals of three β-lactamases: (a) SHV E166A, (b) wild-type SHV-1, and (c) SHV-2.

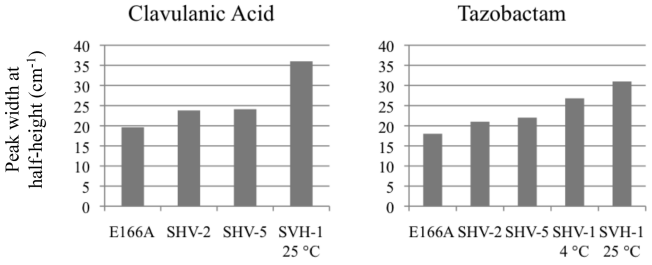

FIGURE 4: Peak widths at half-height for the intense *trans*-enamine stretching feature near 1600 cm^{-1} for clavulanic acid and tazobactam reacting in single crystals of the named enzymes. The complex spectral profile precludes measurements for sulbactam.

studies of biological molecules, broadened band shapes are usually attributed to static and/or dynamic conformational heterogeneity. In a recent study, a strong correlation was observed between Raman bandwidth and X-ray *B*-factors (*18*). Thus, in the instance presented here, the broader peak widths in Figure 4 of the tazo-derived fragments from SHV-1 are ascribed to the existence of multiple forms differing slightly in conformation. Chemically, these have the same parent *trans*-enamine structure; however, a range of slightly different torsional angles in the enamine skeleton effectively broadens the band profile compared to the same feature in the SHV-2 and -5 difference spectra (Figure 4). A second possibility is related to the inhibitor "tails" extending beyond N4. Calculations confirm that extensive vibrational coupling exists between motions in the O=C−C=C−NH fragment and adjacent bonds. Thus, static or dynamic disorder in the tail can also lead to broadening of the band near 1600 cm^{-1}. Regardless, the effect of stabilizing the *trans*-enamine intermediate is to reduce the rate constant for tautomerization to that of the hydrolysis-prone imine. The Raman data show that the *trans*-enamine intermediates of SHV-2 and -5 are in well-defined conformations that undergo only minimal excursions from the mean dihedral angle; and we hypothesize that this increases the intermediate's stability. This trend explains the in vivo and in vitro responses of these ESBLs to tazobactam and clavulanic acid. Unfortunately, a simple band shape analysis is not possible for sulbactam because of the spectral complexity as demonstrated in Figure 1.

Protein Conformational Change. In the difference spectrum of each inhibitor with the extended-spectrum variant SHV-2, the intense features near 1663 and 1678 cm^{-1} are assigned to protein amide I modes that appear due to secondary structural changes occurring upon acylation (Figures 1c, 2c, and 3c). The protein bands are less apparent in the clavulanate−SHV-2 different spectrum because of interference from ligand-associated modes. In the spectrum of native crystals, the amide I profile, 1620−1700 cm^{-1}, contains contributions at different positions from modes due to α-helices, β-sheets, β-strands, and unordered regions of polypeptide. When β-sheet and β-strand features appear in the difference spectra, such as the Raman lines between 1663 and 1676 cm^{-1}, respectively, it indicates a ligand-induced conformational change involving β-structure. SHV-2 contains a single G238S change relative to the wild-type enzyme SHV-1; thus, any additional protein conformation changes that occur from binding the inhibitor to SHV-2 compared to SHV-1 must be attributed to this single amino acid substitution. A high-resolution crystal structure of SHV-2 shows a significant 1−3 Å displacement in the β-strand−turn segment of residues 238−242 compared to SHV-1. The G238S mutation makes this β-strand, which forms one wall of the substrate binding site, more flexible. Consequently, the binding site is more open to newer cephalosporins with large C7 substituents and thereby expands the substrate spectrum of the variant enzyme. We propose that the conformational changes observed in the SHV-2 and SHV-5 difference spectra represent a tightening of the β-structure in the β-strand−turn segment of residues 238−242 that occurs upon acylation by a mechanism-based inhibitor. In turn, this creates a more rigid binding site for the inhibitor and drives the *trans*-enamine intermediate to adopt a more rigid conformation. When oxyimino-cephalosporins, such as cefotaxime and ceftazidime, bind to SHV-2 or SHV-5, the flexible β-strand−turn segment is held in an open conformation to accommodate the large C7 substituents. Thus, we do not observe a conformational change as we do for the small clinically relevant inhibitors. The absence of a conformational change giving rise to features in the 1663−1678 cm^{-1} region is apparent in Figure 5, which shows the Raman difference spectra of SHV-2 with cefotaxime and ceftazidime following a 5 min soak.

Detection of Enamine by Stopped-Flow Ultraviolet Spectroscopy. There are two general findings from the Raman data. (1) Compared to WT, SHV-2 and -5 form relatively more *trans*-enamine (when compared to the relative population levels of imine and *cis*-enamine), and (2) the *trans*-enamine intermediate of tazobactam in SHV-2 and SHV-5 is in a "tighter" conformation than in SHV-1. Additional support for conclusion (1) comes from stopped-flow kinetic studies.

Under pre-steady-state conditions, UV time traces were recorded between 1:1 complexes of tazobactam and SHV-1, -2,

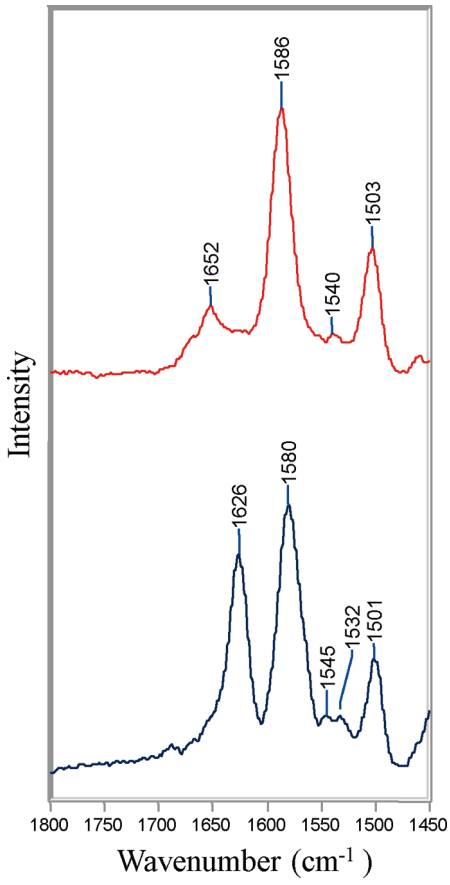

FIGURE 5: Partial Raman difference spectra of cefotaxime (top) and ceftriaxone (bottom) reacting in single crystals of SHV-2. Note the lack of features from 1660 to 1680 cm^{-1}, which indicates that these compounds do not bring about a conformational change in the active site.

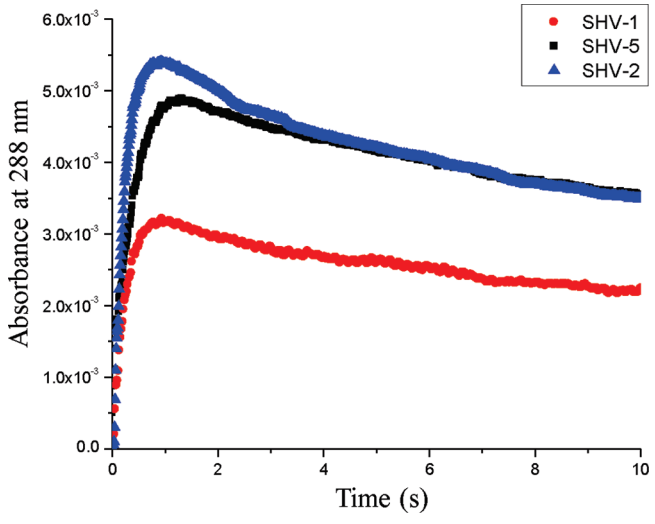

FIGURE 6: Stopped-flow absorption traces for tazobactam reacting with WT SHV-1, SHV-2, and SHV-5 in equimolar ratios. Note the higher absorbance at 288 nm at ~1 s indicates larger enamine populations for SHV-2 and SHV-5.

or -5 β-lactamase. The change in absorbance at 288 nm over 0−10 s is shown for each enzyme in Figure 6. An increase in absorbance at 288 nm is indicative of the formation of an enamine-type intermediate (*25*). The λ_{max} and extinction coefficient of the enamine chromophore do not differ significantly among SHV-1, -2, and -5 (M. Kalp and P. R. Carey, unpublished data); consequently, the traces can be used to compare the amount of enamine formed among the various enzymes. As shown in Figure 6, SHV-2 and -5 form approximately 35% more of the enamine-type intermediate than SHV-1. Studies on the β-lactamase (EC 3.5.2.6) from *Staphylococcus aureus* attributed the biphasic nature of the traces to a *cis*−*trans* isomerization, whereby the first-formed enamine with a UV maximum near 290 nm converts to a stable form of the inactivated enzyme that has a minimum at 275 nm (*26*, *27*). Because the Raman spectra are acquired on the time scale of minutes, the reported isomerization would be near completion by the acquisition of the first Raman spectrum at 2 min.

CONCLUSION

Mention of inhibitor hypersusceptibility is widespread throughout the basic and clinical science literature on ESBLs; however, studies aimed at explaining this phenomenon are lacking. Using two of the most prevalent SHV-type ESBLs, SHV-2 and SHV-5, we show that hypersusceptibility to tazobactam, sulbactam, and clavulanic acid is the direct result of increased stability of the *trans*-enamine intermediate in ESBLs compared to WT. The increased stability, as detected by Raman band shape analysis of the *trans*-enamine's O=C−C=C−NH stretch, slows tautomerization to the hydrolytically labile imine and leads to increased populations of the *trans*-enamine acyl−enzyme intermediate as determined by both Raman difference spectroscopy and time-resolved UV spectroscopy. As a result, the K_I, or the inhibitor concentration required to produce half-maximal inhibition, is lowered by as much as 50-fold for the mechanism-based inhibitors. While these changes to the kinetic parameters are small, they are sufficient to produce hypersusceptibility as judged by the MICs.

SUPPORTING INFORMATION AVAILABLE

Steady-state kinetic parameters for SHV-1, SHV-2, and SHV-5 with ampicillin and nitrocefin and SHV-2 and SHV-5 with cefotaxime and ceftazidime and difference spectra of SHV-5 with tazobactam, sulbactam, and clavulanic acid. This material is available free of charge via the Internet at http://pubs.acs.org.

REFERENCES

1. Paterson, D. L., and Bonomo, R. A. (2005) Extended-spectrum β-lactamases: A clinical update. *Clin. Microbiol. Rev. 18*, 657–686.
2. Paterson, D. L., Ko, W. C., Von Gottberg, A., Mohapatra, S., Casellas, J. M., Goossens, H., Mulazimoglu, L., Trenholme, G., Klugman, K. P., Bonomo, R. A., Rice, L. B., Wagener, M. M., McCormack, J. G., and Yu, V. L. (2004) International prospective study of *Klebsiella pneumoniae* bacteremia: Implications of extended-spectrum β-lactamase production in nosocomial infections. *Ann. Intern. Med. 140*, 26–32.
3. Paterson, D. L., Ko, W. C., Von Gottberg, A., Mohapatra, S., Casellas, J. M., Goossens, H., Mulazimoglu, L., Trenholme, G., Klugman, K. P., Bonomo, R. A., Rice, L. B., Wagener, M. M., McCormack, J. G., and Yu, V. L. (2004) Antibiotic therapy for *Klebsiella pneumoniae* bacteremia: Implications of production of extended-spectrum β-lactamases. *Clin. Infect. Dis. 39*, 31–37.
4. Rodriguez-Bano, J., and Pascual, A. (2008) Clinical significance of extended-spectrum β-lactamases. *Expert Rev. Anti-Infect. Ther. 6*, 671–683.
5. Kliebe, C., Nies, B. A., Meyer, J. F., Tolxdorff-Neutzling, R. M., and Wiedemann, B. (1985) Evolution of plasmid-coded resistance to broad-spectrum cephalosporins. *Antimicrob. Agents Chemother. 28*, 302–307.
6. Knothe, H., Shah, P., Krcmery, V., Antal, M., and Mitsuhashi, S. (1983) Transferable resistance to cefotaxime, cefoxitin, cefamandole

and cefuroxime in clinical isolates of *Klebsiella pneumoniae* and *Serratia marcescens*. *Infection 11*, 315–317.
7. Jacoby, G. A. (1997) Extended-spectrum β-lactamases and other enzymes providing resistance to oxyimino-β-lactams. *Infect. Dis. Clin. North Am. 11*, 875–887.
8. Jacoby, G. A., and Medeiros, A. A. (1991) More extended-spectrum β-lactamases. *Antimicrob. Agents Chemother. 35*, 1697–1704.
9. Philippon, A., Labia, R., and Jacoby, G. (1989) Extended-spectrum β-lactamases. *Antimicrob. Agents Chemother. 33*, 1131–1136.
10. Livermore, D. M., Canton, R., Gniadkowski, M., Nordmann, P., Rossolini, G. M., Arlet, G., Ayala, J., Coque, T. M., Kern-Zdanowicz, I., Luzzaro, F., Poirel, L., and Woodford, N. (2007) CTX-M: Changing the face of ESBLs in Europe. *J. Antimicrob. Chemother. 59*, 165–174.
11. Livermore, D. M., and Hawkey, P. M. (2005) CTX-M: Changing the face of ESBLs in the UK. *J. Antimicrob. Chemother. 56*, 451–454.
12. Knox, J. R. (1995) Extended-spectrum and inhibitor-resistant TEM-type β-lactamases: Mutations, specificity, and three-dimensional structure. *Antimicrob. Agents Chemother. 39*, 2593–2601.
13. Huletsky, A., Knox, J. R., and Levesque, R. C. (1993) Role of Ser-238 and Lys-240 in the hydrolysis of third-generation cephalosporins by SHV-type β-lactamases probed by site-directed mutagenesis and three-dimensional modeling. *J. Biol. Chem. 268*, 3690–3697.
14. Nukaga, M., Mayama, K., Hujer, A. M., Bonomo, R. A., and Knox, J. R. (2003) Ultrahigh resolution structure of a class A β-lactamase: On the mechanism and specificity of the extended-spectrum SHV-2 enzyme. *J. Mol. Biol. 328*, 289–301.
15. Orencia, M. C., Yoon, J. S., Ness, J. E., Stemmer, W. P., and Stevens, R. C. (2001) Predicting the emergence of antibiotic resistance by directed evolution and structural analysis. *Nat. Struct. Biol. 8*, 238–242.
16. Helfand, M. S., and Bonomo, R. A. (2005) Current challenges in antimicrobial chemotherapy: The impact of extended-spectrum β-lactamases and metallo-β-lactamases on the treatment of resistant Gram-negative pathogens. *Curr. Opin. Pharmacol. 5*, 452–458.
17. Helfand, M. S., Totir, M. A., Carey, M. P., Hujer, A. M., Bonomo, R. A., and Carey, P. R. (2003) Following the reactions of mechanism-based inhibitors with β-lactamase by Raman crystallography. *Biochemistry 42*, 13386–13392.
18. Padayatti, P. S., Helfand, M. S., Totir, M. A., Carey, M. P., Carey, P. R., Bonomo, R. A., and van den Akker, F. (2005) High resolution crystal structures of the *trans*-enamine intermediates formed by sulbactam and clavulanic acid and E166A SHV-1 β-lactamase. *J. Biol. Chem. 280*, 34900–34907.
19. Padayatti, P. S., Helfand, M. S., Totir, M. A., Carey, M. P., Hujer, A. M., Carey, P. R., Bonomo, R. A., and van den Akker, F. (2004) Tazobactam forms a stoichiometric trans-enamine intermediate in the E166A variant of SHV-1 β-lactamase: 1.63 Å crystal structure. *Biochemistry 43*, 843–848.
20. Totir, M. A., Padayatti, P. S., Helfand, M. S., Carey, M. P., Bonomo, R. A., Carey, P. R., and van den Akker, F. (2006) Effect of the inhibitor-resistant M69V substitution on the structures and populations of *trans*-enamine β-lactamase intermediates. *Biochemistry 45*, 11895–11904.
21. Hujer, A. M., Hujer, K. M., and Bonomo, R. A. (2001) Mutagenesis of amino acid residues in the SHV-1 β-lactamase: The premier role of Gly238Ser in penicillin and cephalosporin resistance. *Biochim. Biophys. Acta 1547*, 37–50.
22. Carey, P. R. (2006) Spectroscopic characterization of distortion in enzyme complexes. *Chem. Rev. 106*, 3043–3054.
23. Kalp, M., Totir, M. A., Buynak, J. D., and Carey, P. R. (2009) Different intermediate populations formed by tazobactam, sulbactam, and clavulanate reacting with SHV-1 β-lactamases: Raman crystallographic evidence. *J. Am. Chem. Soc. 131*, 2338–2347.
24. Sulton, D., Pagan-Rodriguez, D., Zhou, X., Liu, Y., Hujer, A. M., Bethel, C. R., Helfand, M. S., Thomson, J. M., Anderson, V. E., Buynak, J. D., Ng, L. M., and Bonomo, R. A. (2005) Clavulanic acid inactivation of SHV-1 and the inhibitor-resistant S130G SHV-1 β-lactamase. Insights into the mechanism of inhibition. *J. Biol. Chem. 280*, 35528–35536.
25. Bush, K., Macalintal, C., Rasmussen, B. A., Lee, V. J., and Yang, Y. (1993) Kinetic interactions of tazobactam with β-lactamases from all major structural classes. *Antimicrob. Agents Chemother. 37*, 851–858.
26. Cartwright, S. J., and Coulson, A. F. (1979) A semi-synthetic penicillinase inactivator. *Nature 278*, 360–361.
27. Rizwi, I., Tan, A. K., Fink, A. L., and Virden, R. (1989) Clavulanate inactivation of *Staphylococcus aureus* β-lactamase. *Biochem. J. 258*, 205–209.